Current Plant Biology 41 (2025) 100442

Contents lists available at ScienceDirect

Current Plant Biology

journal homepage: www.elsevier.com/locate/cpb

Comparative transcriptome and co-expression network analysis uncovers the regulatory mechanism of silicon-induced soybean defense against charcoal rot disease

Pravin Jadhav [a,*], Sayali Magar [a], Parva Sharma [b], Umesh Shinde [a], Eknath Vaidya [a], Mangesh Moharil [a], Sarika Jaiswal [b], Satish Nichal [d], Rajiv Ghawade [d], Mir Asif Iquebal [b], Prashant Kawar [e], Pritam Jadhav [e], Sanjay Sakhare [a], Rameshwar Ghorade [a], Rupesh Deshmukh [f], Humira Sonah [f], Dinesh Kumar [b], Vineet Kumar [g], Vilas Kharche [h], Shyamsunder Mane [c]

[a] Biotechnology Centre, Department of Agricultural Botany, Dr. Panjabrao Deshmukh Krishi Vidyapeeth, Akola, Maharashtra 444104, India
[b] Division of Agricultural Bioinformatics, ICAR-Indian Agricultural Statistics Research Institute, New Delhi, India
[c] Department of Plant Pathology, Dr. Panjabrao Deshmukh Krishi Vidyapeeth, Akola, Maharashtra 444104, India
[d] Regional Research Center on Soybean, Dr. Panjabrao Deshmukh Krishi Vidyapeeth, Akola, Amravati, Maharashtra 444601, India
[e] ICAR-Directorate of Floricultural Research, College of Agriculture, Pune, Maharashtra 411 005, India
[f] Department of Biotechnology, Central University of Haryana, Mahendragarh 123029, India
[g] ICAR-Indian Institute of Soybean Research, Indore, Madhya Pradesh 452001, India
[h] Directorate of Research, Dr. Panjabrao Deshmukh Krishi Vidyapeeth, Akola, Maharashtra 444104, India

ARTICLE INFO

Keywords:
Charcoal rot
Macrophomina phaseolina
Potassium silicate
RNA-seq
Soybean

ABSTRACT

Soybean (*Glycine max* L.) is highly susceptible to charcoal rot caused by the soil-borne pathogen *Macrophomina phaseolina*, which can reduce yields by up to 70 %. Effective control methods are lacking, and information on managing the disease is limited. This study investigates how potassium silicate (1.7 mM K_2SiO_3) enhances soybean resistance to charcoal rot. The treatment significantly improved plant health, reducing the mortality rate of the susceptible genotype TAMS-38 from 69.7 % to 9 %. RNA sequencing revealed 3106 differentially expressed genes linked to disease resistance. Resistant genotypes showed upregulation of genes involved in key defense pathways, enhancing resistance mechanisms against charcoal rot including Pathogenesis-Related Protein 1 (PR1) for Systemic Acquired Resistance (SAR) and Salicylic Acid (SA) pathway, Stress-induced protein H4 for Heat Shock Protein (HSP) Pathway, disease resistance proteins for *Resistance* gene and Mitogen-Activated Protein Kinase (MAPK) pathways, pleiotropic drug resistance proteins for detoxification, basic secretory protein (BSP) domain for cell wall reinforcement, NRT1/PTR FAMILY 2.13 for nutrient management, receptor-like kinases for pathogen detection, Pruav 1 for resistance, Dehydration responsive element-binding protein 3 (DREB3) for abscisic acid (ABA) signalling in drought, and chitinase class I precursor for fungal cell wall breakdown. A total of 41 key differentially regulated genes were identified, with 8 validated by qRT-PCR, showing potential for genetic improvement and breeding. These findings provide a basis for developing strategies to combat charcoal rot and improve soybean resilience against *Macrophomina phaseolina*.

1. Introduction

Soybean (*Glycine max* L.) is economically significant due to its high protein and oil content, but its productivity is challenged by various biotic and abiotic stresses [18]. Among these, charcoal rot disease caused by *Macrophomina phaseolina* poses a major threat, leading to a 77 % reduction in soybean production in Indian fields [5,44]. *Macrophomina phaseolina* is a soil-borne fungus that infects over 500 host species [43]. It spreads from the roots to the stems, producing black microsclerotia that block vascular tissues, impairing growth and

* Corresponding author.
E-mail address: jpraveen26@yahoo.co.in (P. Jadhav).

https://doi.org/10.1016/j.cpb.2025.100442
Received 26 September 2024; Received in revised form 7 January 2025; Accepted 15 January 2025
Available online 20 January 2025

reducing yield [21]. Symptoms of infection usually appear after flowering and peak during critical growth stages (R5-R7) in soybeans. Although various management strategies, such as cultural practices, fungicide applications, and biological controls, have been tried, they have not been broadly effective against *Macrophomina phaseolina* [30]. No plant species is completely resistant to *Macrophomina phaseolina*; however, soybean genotypes like DT97–4290 and PI 567562 A have shown moderate resistance [10]. In India, the 'Suvarna Soya' (AMS-MB-05–18) variety, resistant to *Macrophomina phaseolina*, was developed through collaboration between Dr. Panjabrao Deshmukh Krishi Vidyapeeth, Akola, and the Bhabha Atomic Research Centre, Trombay, and released nationally in 2019. However, the molecular responses of soybean to *Macrophomina phaseolina* are not well understood, underscoring the need to identify differentially expressed genes that confer resistance. Similarly, silicon (Si) has garnered significant attention for its role in enhancing plant resilience against fungal pathogens. Silicon accumulation in plant cells is linked to improved stress tolerance [25,41], and applying exogenous silicon has been shown to effectively reduce fungal infections in a variety of crops [39,42]. Plants mainly absorb silicon as monosilicic acid ($Si(OH)_4$), which is poorly mobile in the soil at a solubility of pH 9 and concentrations below 2 mM. As a result, silicon fertilizers are typically applied to the roots at concentrations up to 2 mM [16,29]. In the present investigation, the 1.7 mM silicon concentration was selected based on results from a pilot experiment that tested 0.7 mM, 1.7 mM, and 2.0 mM concentrations, along with a control. The 1.7 mM concentration exhibited superior performance in disease mitigation, silicon uptake, and biochemical and molecular responses under treated conditions. These findings align with those reported by Mandlik et al. [29]. Accordingly, 1.7 mM was chosen for the differential gene expression (DEG) study to enable a focused and meaningful analysis of its role in resistance mechanisms. Previous studies have demonstrated the utility of transcriptomic approaches, like RNA-Seq, for identifying molecular markers of disease resistance [11, 52]. The rapidly advancing field of transcriptomics allows for a comprehensive understanding of the complex plants - microbe interactions [32]. However, there is still a knowledge gap regarding the molecular mechanisms underlying soybean resistance to *Macrophomina phaseolina* and the role of silicon in this process. This investigation aims to address these gaps by investigating the molecular basis of soybean's defense mechanisms against *Macrophomina phaseolina* and the impact of silicon treatment on gene expression related to charcoal rot resistance.

2. Materials and methods

2.1. Plant material and characterization of fungus

The experimental genotypes AMS-MB-5–18 (Suvarna Soya, resistant variety) and TAMS-38 (highly susceptible) were developed by Dr. Panjabrao Deshmukh Krishi Vidyapeeth, Akola through mutation breeding, in collaboration with the Bhabha Atomic Research Center, Trombay, Mumbai during 2019. For disease screening, *Macrophomina phaseolina* was isolated from an infected soybean field and validated at morphological and molecular level. The soil samples were collected from a soybean field affected by charcoal rot caused by *Macrophomina phaseolina* at the sick plot maintained for screening charcoal rot resistance in soybean at the Regional Research Center on Soybean, Amravati. The pathogen was isolated using the serial dilution technique and cultured on Potato Dextrose Agar (PDA) medium. Its identity was confirmed microscopically using lactophenol cotton blue staining, following the protocol of Almomani et al. [4]. Genomic DNA from the pathogen was extracted using the DNAzol method [45], amplified with Internal Transcribed Spacer 1/4 (ITS1/4) primers, sequenced, and analyzed through Basic Local Alignment Search tool (BLAST). The sequence data has been submitted to National Center for Biotechnology Information (NCBI) for reference.

2.2. In-vitro screening of soybean genotypes for silicon effectiveness against Macrophomina phaseolina

In-vitro screening for an RNA sequencing (RNA-seq) study was performed to evaluate the impact of silicon treatment on soybean genotypes. The mass multiplication method was utilized to infect soybean plants under *in vitro* condition. Fully grown cultures of *Macrophomina phaseolina* on PDA were transferred onto sterilized sorghum seeds, which served as the substrate for fungal growth over 21 days. The resulting mass-multiplied fungal inoculum was mixed with sterile soil at a 1:3 ratio (one part fungal-infected sorghum seeds to three parts sterile soil) and used for the *in vitro* infection experiment. Using the pot culture method, both resistant and susceptible genotypes were grown in pots and inoculated with *Macrophomina phaseolina* (strain Akola-01). The *in-vitro* studies were conducted in three biological replications of AMS-MB-5–18 (Suvarna Soya, resistant variety) and TAMS-38 (highly susceptible variety) at the Biotechnology Centre, Department of Agricultural Botany, Dr. Panjabrao Deshmukh Krishi Vidyapeeth, Akola. The pots were maintained in a climate-controlled greenhouse at 30–35°C. Five treatments were assessed: T1 (Control), T2 (Silicon control), T3 (Charcoal rot), T4 (0.7 mM potassium silicate), and T5 (1.7 mM potassium silicate). After observing the *in- vitro* results at the V6-R7 growth stage, the promising treatments (T1, T3 and T5) further selected for RNA-seq study. Silicon uptake and accumulation were analysed using Scanning Electron Microscopy (SEM) and Energy Dispersive X-ray Spectroscopy (EDX), while RNA sequencing was performed to explore gene expression profiles.

2.3. Uptake and accumulation of K_2SiO_3

Tissue samples from resistant and susceptible genotypes, subjected to control, charcoal rot, and 1.7 mM potassium silicate treatments, were analysed 45 days' post seedling. Scanning Electron Microscopy (SEM) and Energy Dispersive X-ray Spectroscopy (EDX) were conducted using a Jeol JSM-IT300 SEM with an EDX analyser (EDAX Octane Plus). Silicon distribution was assessed and reported as weight percentages of total Si, processed with TEAM Enhanced ver. 4.3 software. Additionally, RNA-seq was employed for transcriptomic analysis to explore how silicon treatment affects responses to *Macrophomina phaseolina* infection in different genotypes.

2.4. RNA sequencing

The RNA sequencing data for total six biological leaf tissue samples (S1-S6) comprising resistant and susceptible soybean genotypes were taken. The soil was first inoculated with *Macrophomina phaseolina* prior to sowing the soybean seeds. Following sowing, only the designated treatment pots were irrigated with 250 mL of a K_2SiO_3 solution weekly, while the control pots were irrigated with an equivalent volume (250 mL) of normal water. This irrigation regimen was maintained as required throughout the experimental period to ensure consistent application of the silicon treatment and adequate watering for all plants. The samples include treatments designated as BioSample: **SAMN37757654**: **S1-** Control (T1 of TAMS-38 in *in-vitro* experiment) (Normal watering without charcoal rot infection); **SAMN37757655**: **S2-** Charcoal rot (T3 of TAMS-38 in *in-vitro* experiment) (Charcoal rot infected soil with normal watering); **SAMN37757656**: **S3-** 1.7 mM potassium silicate (T5 of TAMS-38 in *in-vitro* experiment) (Charcoal rot-infected soil treated with 1.7 mM K_2SiO_3 via water drenching); **SAMN37757657**: **S4-** Control (T1 of AMS-MB-5–18 in *in-vitro* experiment) (Normal watering without charcoal rot infection); **SAMN37757658**: **S5-** Charcoal rot (T3 of AMS-MB-5–18 in *in-vitro* experiment) (Charcoal rot infected soil with normal watering) and **SAMN37757659**: **S6-**1.7 mM potassium silicate (T5 of AMS-MB-5–18 in *in-vitro* experiment) (Charcoal rot-infected soil treated with 1.7 mM K_2SiO_3 via water drenching).

Plants were kept in the greenhouse until disease symptoms emerged. Leaf tissue samples were collected 45 days' post seedling at R1 stage (beginning bloom stage, marked by the first open flower on the main stem, signalling the start of reproductive growth). Studying differential gene expression (DGE) at the R1 stage is more biologically relevant for capturing the plant's active response to *Macrophomina phaseolina* infection. At this stage, the plant's defense mechanisms are fully engaged, and the interplay between pathogen invasion and host resistance is at its peak. Analysing gene expression at this stage allows for the identification of genes that are upregulated or downregulated in response to infection, providing valuable insights into the molecular pathways involved in stress signalling, pathogen recognition, and defense activation. By focusing on the R1 stage, the study ensures that the actual transcriptional response to fungal infection is accurately recorded, enhancing the reliability of identifying resistance-associated genes and pathways [33]. Tissue samples from both genotypes were rapidly frozen in liquid nitrogen immediately after collection stored at −80°C and used for RNA isolation.

RNA isolation was performed following the manufacturer's protocol for the Spectrum™ Total Plant RNA Kit (Sigma-Aldrich), and 250 ng of total RNA was used for mRNA amplification with the NEB Next Poly(A) mRNA Magnetic Separation Module. Sequencing data were generated using Illumina HiSeq, and mRNA libraries were prepared with the NEB Next Ultra™ II RNA Library Prep Kit. The Illumina HiSeq was performed using HiSeq 2000 on three biological replicates of six samples.

2.5. Transcriptome data processing

Raw reads were quality-checked and processed using Trimmomatic v0.39 [7] to remove sequencing adapters and low-quality reads. Clean reads were stored and analysed with FASTQC-0.11.8 [6]. Transcriptome assembly was conducted using Trinity assembler v2.5.1 [14] for de novo assembly, while the reference-based assembly employed the 'Tuxedo2' protocol (HISAT2 followed by StringTie2). Comparisons between de novo and reference-based assemblies were performed using BLAST+ [8], with the *Glycine max* reference model from Ensembl (http://ftp.ensemblgenomes.org/pub/plants/release-53/fasta/glycine_max/dna/) and the corresponding annotation file (http://ftp.ensemblgenomes.org/pub/plants/release-53/gtf/glycine_max/). The de novo assembly was utilized to identify novel differentially expressed transcripts, transcription factors, variants, and gene regulatory networks.

2.6. Identification of differentially expressed genes (DEGs)

Differentially Expressed Genes (DEGs) were identified using the Trinity tool script. Transcript quantification was performed with RNA-Seq by Expectation Maximization (RSEM) [24], which maps clean reads to the de novo transcriptomic assembly with Bowtie2 [23]. DEGs were detected using a p-value threshold (<0.005) and analyzed with False Discovery Rate (FDR). Significant DEGs were defined with FDR < 0.001, p-value < 0.05, and log2 fold change $\pm$ 2, using the edgeR algorithm [40]. The analysis was conducted across nine condition pairs: (1) susceptible-control *vs* resistant-control, (2) susceptible-control *vs* susceptible-infected, (3) susceptible-control *vs* susceptible-treated, (4) susceptible-infected *vs* resistant-infected, (5) susceptible-treated *vs* resistant-treated, (6) resistant-control *vs* resistant-infected, (7) resistant-control *vs* resistant-treated, (8) resistant-infected *vs* resistant-treated, and (9) susceptible-infected *vs* susceptible-treated.

2.7. Functional annotation, GO enrichment, and transcription factor identification

Functional and Gene Ontology (GO) annotation of the transcripts was conducted using Blast2GO Pro ver 3.1, focusing on biological processes, molecular functions, and cellular components. Kyoto Encyclopaedia of Genes and Genomes (KEGG) pathways and enzyme classes were also identified [9]. KEGG and GO enrichment analyses were performed to identify the most significant pathways and terms [20]. GO enrichment for all upregulated and downregulated DEGs across nine conditions was carried out using Fisher's Exact Test in Blast2GO. Pathway enrichment was based on KEGG pathways identified in DEGs. Transcription factors (TFs) were identified using a BlastX search with E-value < 1e-03 against the Plant TFDB database for all DEGs from the nine datasets [19].

2.8. Variant identification

Biomarkers such as Simple Sequence Repeat (SSRs) and nucleotide polymorphisms were identified. SSRs were detected in de novo assembled transcripts using MISA, including mono-, di-, tri-, tetra-, penta-, and hexanucleotide repeats. Primers for SSRs were designed with Primer3, with annealing temperatures ranging from 57°C to 63°C and primer sizes from 15 to 28 nucleotides. Nucleotide polymorphisms, including Single Nucleotide Polymorphism (SNPs), insertions/deletions InDels, and complex structures, were called using Freebayes. Clean reads were mapped to the transcriptome using Bowtie2, and alignment files were pre-processed with SAMtools for sorting, duplicate removal, and indexing. Variant calling was performed with Freebayes using stringent parameters (minimum mapping quality $\geq$ 20 and minimum base quality $>$ 20).

2.9. Gene regulatory networks

Cytoscape version 3.9.1 was used to construct and visualize gene regulatory networks (GRNs). 'Housekeeping genes,' 'uncharacterized proteins,' and 'similar genes' were excluded from the GRN. DEGs with high log fold changes were used for network construction, with gene correlations calculated using the Pearson Correlation Coefficient. Normalized expression values from all nine conditions were utilized. Hub genes were identified based on network centrality, topology, and node degree.

2.10. Soybean online database resource

To make current research data accessible to the scientific community, we have developed the Soybean Transcriptome Database for charcoal rot (STDbCr). This online resource provides comprehensive information, including transcript annotations, DEGs, transcription factors, biomarkers, and their primers. Developed using the LAMP protocol (Linux Apache MySQL PHP), the database is freely available for academic use at http://backlin.cabgrid.res.in/stdbcr/.

2.11. q-RT-PCR validation

Total RNA was isolated, and cDNA was synthesized using a cDNA synthesis kit (Takara, Japan). Calcium dependent protein kinase (CDPK) (gene cons 15) was used as an internal control [27]. Primers were designed with Primer3 software, and their efficiency was validated. Quantitative reverse transcription polymerase chain reaction (qRT-PCR) was performed with a QIAquant Real-Time Thermal Cycler at ICAR-DFR, Pune, using FastStart SYBR Green Master Mix. Expression levels were calculated using the ΔΔCT method and represented as fold change ($2^{-\Delta\Delta CT}$) [28].

3. Results

3.1. Molecular and morphological characterization of Macrophomina phaseolina

Molecular characterization was conducted to verify the *Macrophomina phaseolina* inoculum for the RNA-seq study. Sequencing of fungal DNA from diseased soybean plants identified the pathogen as

Macrophomina phaseolina, with 96.65 % similarity confirmed via ITS1/4 primer amplification and BLAST analysis. The sequence data is made available in the NCBI database under accession number MZ823608.1 (https://www.ncbi.nlm.nih.gov/search/all/?term=MZ823608.1). Morphological characteristics were confirmed under a microscope using lactophenol cotton blue. Fig. 1 shows: colonies on potato dextrose agar (1 A), aerial hyphal network (1B), PCR amplicon size (1 C), light micrographs of pycnidium and sclerotia (1D-E), and hyphal networks on soybean stems (1F-G). Additionally, video footage (https://youtube.com/shorts/t1iT5Hic2_M) documented the fungus penetrating soybean roots, establishing a foothold within 3–4 hours.

A- Colonies of *Mp* grown on potato dextrose agar after 7 days of incubation; B- Aerial hyphal network of *Mp* stained with cotton blue; C- Molecular characterization of *Mp* a using ITS1/4 primer, revealing a band size of 430 bp; D&E- light micrograph of globus pycnidium and sclerotia alongside hyphae; F&G- Longitudinal cut section of a soybean stem, revealing sclerotia and a web-like network of hyphae characteristic of *Mp* infection, predominantly observed on the inner side of the soybean stem.

3.2. *In-vitro screening of soybean genotypes against charcoal rot disease using potassium silicate*

The RNA-seq study assessed the impact of silicon treatment on soybean genotypes under controlled conditions, revealing that silicon enhances tolerance to fungal infections. Significant differences were observed between resistant and susceptible genotypes (Fig. 2A). For the TAMS-38 genotype, control plants (T1) and those infected with charcoal rot (T3) exhibited poor growth, with symptoms like reduced height, low germination, and withering. In contrast, plants treated with 1.7 mM K_2SiO_3 (T5) showed improved growth and resilience, highlighting silicon's role in enhancing tolerance to charcoal rot. Infected seeds (T3) were of poor quality, with blackening and rot, whereas silicon-treated seeds (T5) were healthy, akin to non-infected seeds (T1) (Fig. 2B-I). The AMS-MB-5–18 genotype, inherently resistant to charcoal rot, showed minimal impact from the disease but benefited from silicon treatment, which improved growth parameters (Fig. 2A-II). Examination of TAMS-38 stems (Fig. 2C) revealed severe infection in untreated plants (T3), with significant blackening and sclerotia presence, while silicon-treated plants (T5) had reduced infection. Control plants (T1) showed no infection. SEM analysis of silicon accumulation confirmed that increased silicon deposition corresponded with decreased disease incidence.

A: Comparative *in-vitro* screening of soybean genotypes; A-I: susceptible genotype (TAMS-38); A-II: resistant genotype (AMS-MB-05–18) for Si effect against charcoal rot; T1: Control; T2: Silicon control; T3: Charcoal rot; T4: 0.7 mM Potassium silicate; T5: 1.7 mM Potassium silicate. B: Symptoms of charcoal rot revealed presence of fungal sclerotia in T1 to T5 of TAMS-38 susceptible genotype charcoal coloured growth observed in infected soybean stem prominently in T3 whereas, T4 & T5 observed with minor infection of C.R.; C: Seeds development in susceptible and resistant soybean genotypes with treatment and without treatment.

3.3. *Scanning electron microscopy of silicon accumulation in soybean leaves and roots*

SEM analysis of the TAMS-38 and AMS-MB-05–18 genotypes under various treatments revealed distinct silicon accumulation patterns (Fig. 3, images 3 A & 3B). Control plants (T1) showed baseline silicon levels around 0.8 %, with normal leaf and root morphology and minimal silicon deposition (Fig. 3, images A3 & B3 for leaves; A5 & B5 for roots). Infected plants not treated with silicon (T3) had slightly lower silicon levels at 0.7 %, with roughened leaf surfaces but no significant silicon accumulation (Fig. 3, images A8 & B8 for leaves; A10 & B10 for roots). In contrast, silicon-treated plants (T5) showed substantial silicon deposition, with levels reaching 1.8 %. SEM images indicated notable silicon accumulation on leaf surfaces, especially in trichomes, and within root vascular tissues (Fig. 3, images A13 & B13 for leaves; A15 & B15 for roots). EDX mapping confirmed this increase, correlating with

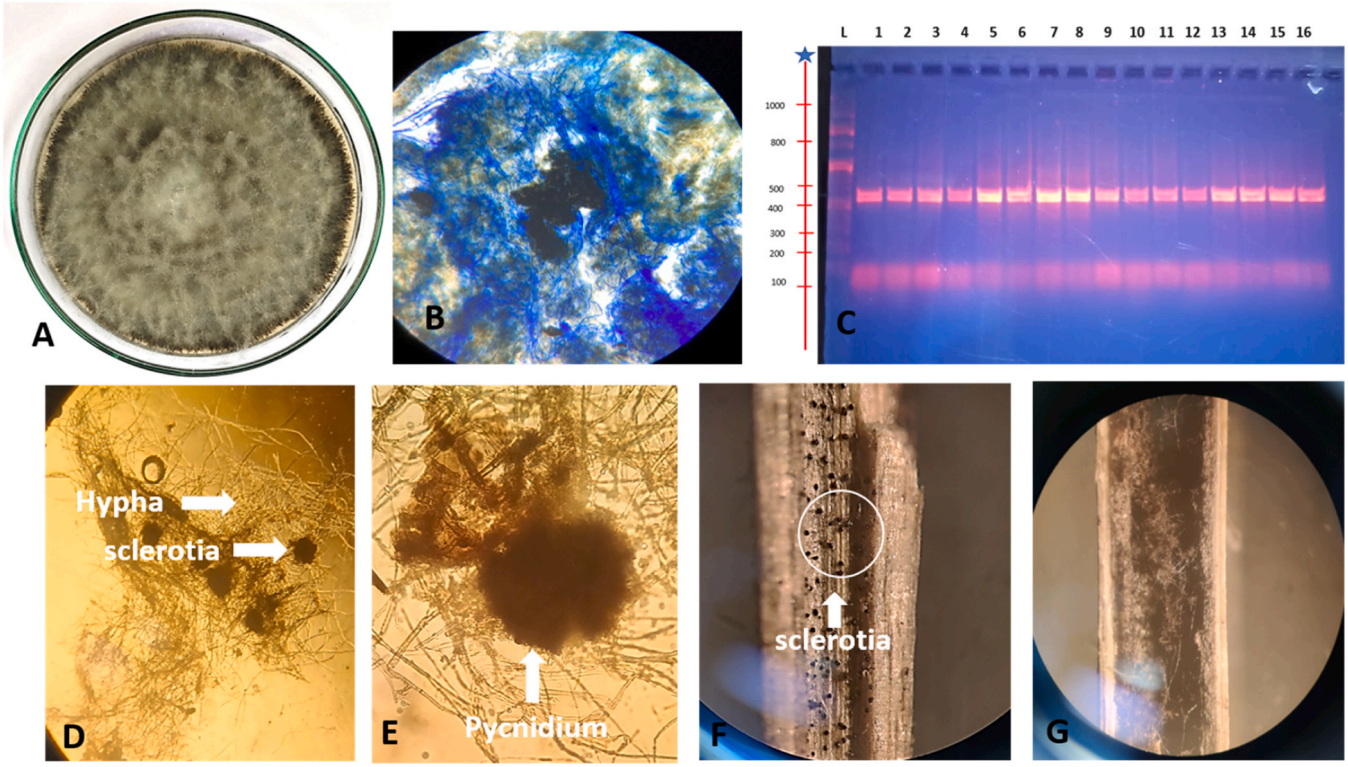

Fig. 1. Molecular and morphological characteristics of *Macrophomina phaseolina*.

Fig. 2. *In-vitro* screening for charcoal rot disease under potassium silicate treatment.

improved plant health and resistance to charcoal rot. Silicon enhances resistance by forming physical barriers that impede fungal invasion and strengthen cell walls. These findings underscore the significant correlation between silicon deposition and increased resistance in the susceptible genotype TAMS-38, with images A11 demonstrating healthier growth compared to A1 and infected plants (A6). This observation sets the foundation for the subsequent transcriptomic analysis.

3.4. RNA-Seq analysis of soybean defense mechanisms against Macrophomina phaseolina and the effect of silicon supplementation

3.4.1. Raw data Pre-processing and transcriptome assembly

Sequencing results for six leaf tissue samples (S1-S6) from two contrasting soybean varieties yielded 150 base pair reads. The read pairs were as follows: susceptible control (16,933,056), susceptible infected (17,224,957), susceptible treated (20,157,934), resistant control (17,666,231), resistant infected (17,678,885), and resistant treated (23,959,344). A summary of reads before and after trimming is in Supplementary Table 1. After quality filtering, 102,074,449 high-quality reads were used for transcriptome assembly, resulting in 227,790 genes and 410,789 transcripts via the Trinity assembler. The average contig length was 999.38 base pairs, with a GC content of 40.53 % and an N50 value of 1894 base pairs. In the reference-based assembly, 117,311 transcripts had an N50 value of 2.699 Kb. Supplementary Table 2 compares both assemblies. BLAST+ comparison revealed 110,173 common transcripts, with the de-novo assembly containing 48.36 % and the reference-based assembly 94.12 %, indicating unique transcripts in the de-novo assembly. The de-novo assembly produced 117,617 new transcripts, compared to 6880 in the reference-based assembly (Fig. 4).

3.4.2. Differentially expressed genes (DEGs) identification

In this study, significant DEGs with parameters of FDR and p-value < 0.05 and log2 fold change > 2 were identified across nine comparison sets, as shown in Fig. 5. A total of 2079 unique DEGs (out of 3106 total) were distributed among these sets. The DEGs per comparison set were: 354 (susceptible-control vs resistant-control), 21 (susceptible-control vs susceptible-infected), 318 (susceptible-control vs susceptible-treated), 929 (susceptible-infected vs resistant-infected), 412 (susceptible-treated vs resistant-treated), 206 (resistant-control vs resistant-infected), 41 (resistant-control vs resistant-treated), 519 (resistant-infected vs resistant-treated), and 306 (susceptible-infected vs susceptible-treated) (Fig. 5, Supplementary Sheet 1). Fig. 6 presents a heatmap of the Spearman correlation matrix based on Trimmed Mean of M component (TMM) -normalized Fragments Per Kilobase per Million mapped fragments (FPKM) values, and Supplementary Fig. 1 shows hierarchical clustering of DEGs and samples. Supplementary Fig. 2 includes MA and volcano plots for individual comparisons. Fig. 7 displays the shared and unique DEGs. The highest number of DEGs (531) were observed in the susceptible-infected vs resistant-infected comparison, indicating strong resistance gene expression in the resistant variety.

The second highest (215) was seen in susceptible-treated vs resistant-treated, reflecting treatment-sensitive genes. Unique DEGs were 154, 5, 79, 531, 215, 30, 11, 207, and 85 for each comparison set, respectively. Additionally, 531 genes were common in two sets, 203 in three sets, 24 in four sets, 3 in five sets, and 1 in seven sets (Fig. 7).

3.5. Defence related genes

To establish a baseline, gene expression profiles from healthy, infected, and 1.7 mM Si-treated samples were used. Genes showing a twofold or greater difference in expression between infected and control samples ($p < 0.001$) were considered differentially expressed (DEGs) (Table 1).

Analysis of 3106 DEGs identified 41 key genes, including pathogenesis-related proteins, stress-induced proteins, and disease resistance proteins. These genes were upregulated in resistant soybean genotypes and downregulated in susceptible ones, suggesting their

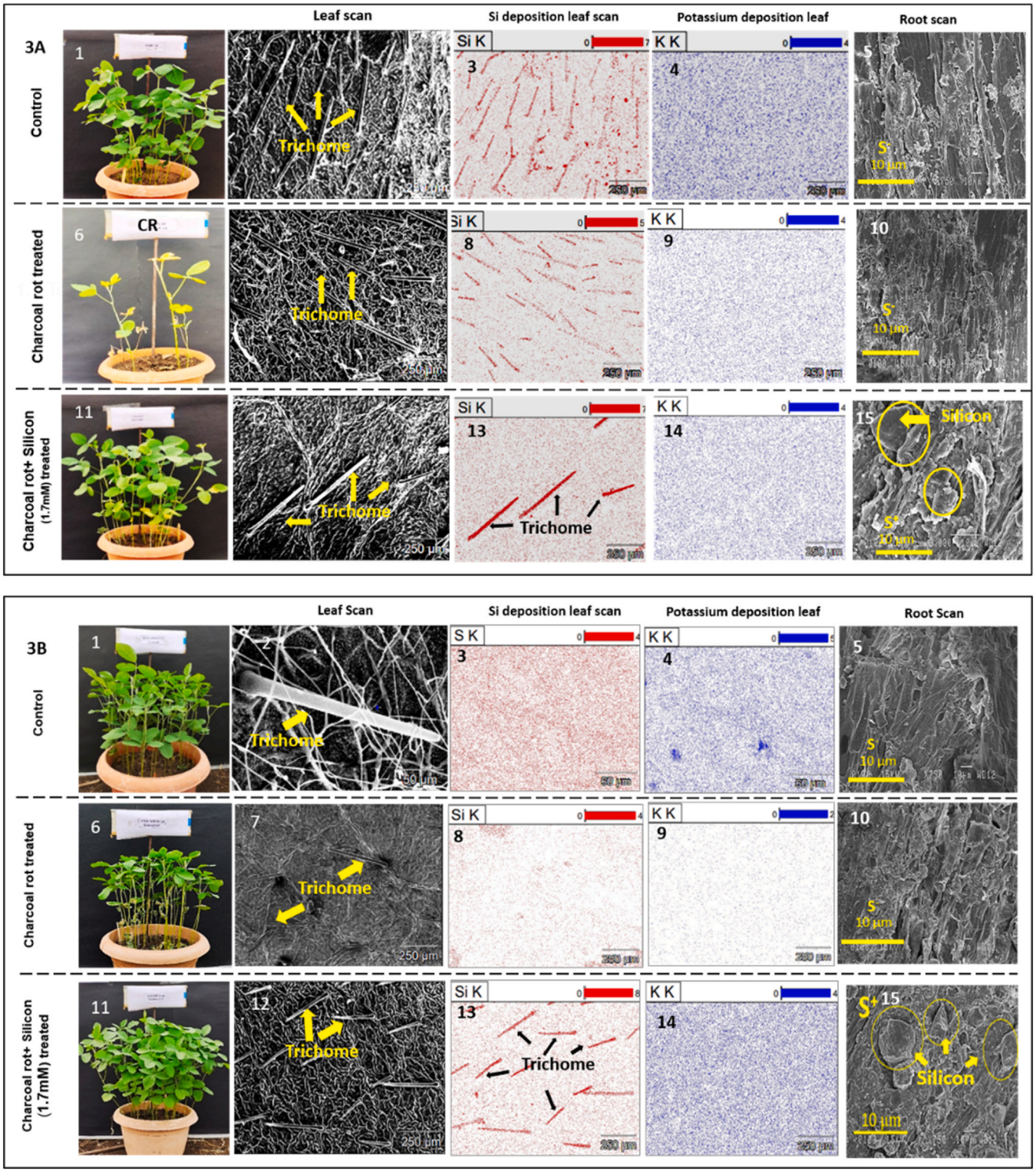

Fig. 3. Comparative study of SEM and EDX analysis for uptake and accumulation of silicon in soybean genotype cv., (3 A): TAMS-38, (3B): AMS-MB-5–18, tissue leaf and root.

potential for enhancing charcoal rot resistance. Specifically, proline-rich protein and gibberellin-regulated protein were upregulated in the susceptible genotype (TAMS-38) but downregulated with silicon treatment, while programmed cell death protein showed the opposite pattern. In resistant infected plants, genes like LRR receptor-like serine/threonine-protein kinase and ethylene-responsive transcription factor ABR1 were upregulated, enhancing immunity. Conversely, genes such as alpha-amylase inhibitor and lipid transport were downregulated. In resistant treated plants, ORF16-lacZ fusion protein and putative membrane protein were increased, while inositol-3-phosphate synthase and NAC domain protein were downregulated, highlighting the effectiveness of Si application. Susceptible infected plants had elevated senescence-associated protein and zinc finger protein ZAT10-like, whereas susceptible treated plants showed upregulation of Protein SRC1-like and Early

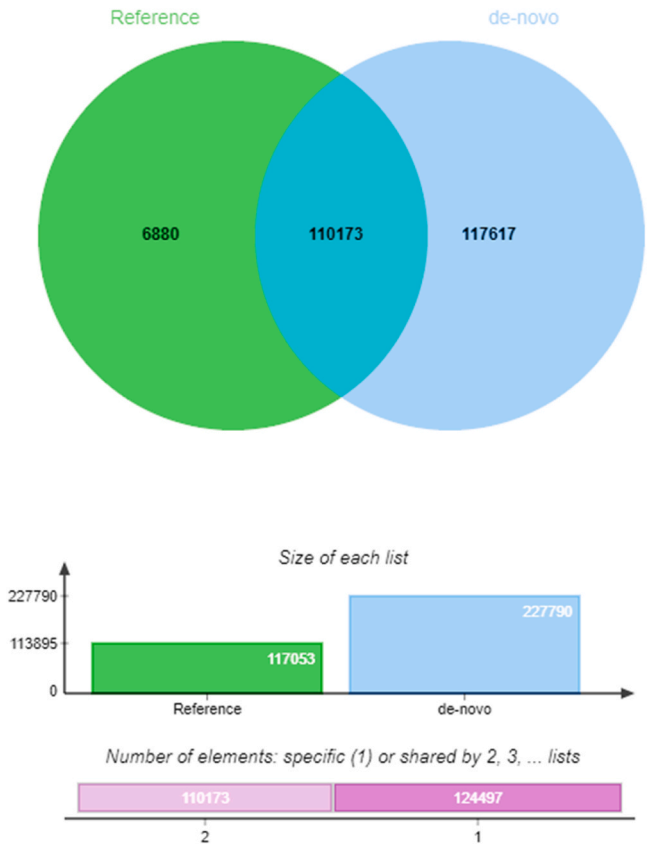

Fig. 4. Comparison of reference and *de-novo*-based assemblies in *Macrophomina phaseolina*.

Nodulin-Like Protein 1 isoform B, but downregulation of Proline-Rich Protein 2 and Gibberellin-Regulated Protein 6. Many genes in susceptible treated plants were associated with hypothetical proteins. Carbonic anhydrase, chloroplastic isoform 1, was increased in susceptible plants but downregulated in resistant ones. RNA-binding protein 12 was upregulated in susceptible plants, suggesting a link to disease development. Auxin-binding protein ABP19a-like was differentially regulated between resistant and susceptible plants. Overall, the findings indicate that upregulation of defense-related genes and enzymes enhances resistance to *Macrophomina phaseolina* without adversely affecting plant growth, and that silicon acts as a priming agent to improve response to pathogen attacks.

3.6. Homology search, annotation, functional characterization and transcription factor identification

All sequences from the nine comparison sets were analyzed for homology using Blast2GO. The highest similarity was found with Glycine soja (>1250 sequences), followed by *Glycine max* (>1150 sequences), indicating their phylogenetic relatedness (Supplementary Fig. 3). Gene ontology (GO) classification of all DEGs was performed for each comparison set: (1) susceptible-control vs resistant-control, (2) susceptible-control vs susceptible-infected, (3) susceptible-control vs susceptible-treated, (4) susceptible-infected vs resistant-infected, (5) susceptible-treated vs resistant-treated, (6) resistant-control vs resistant-infected, (7) resistant-control vs resistant-treated, (8) resistant-infected vs resistant-treated, and (9) susceptible-infected vs susceptible-treated. The identified GO terms for each set are listed in Supplementary Sheet 2 (Total: CC-MF-BP): (1) 382:61–163–158, (2) 54:14–22–18, (3) 390:65–158–167, (4) 635:78–279–278, (5) 584:94–210–280, (6) 201:30–97–74, (7) 70:11–34–25, (8) 422:54–184–184, (9) 426:64–176–186. Most transcripts annotated under cellular components were associated with the membrane ontology, specifically the "integral component of membrane" (GO:0016021) and "membrane" (GO:0016020). The most common molecular function was "transferase activity" (GO:0016740), while "regulation of transcription" (GO:0006355) was the top biological process, followed by "transmembrane transport" (GO:0055085) (Fig. 8).

GO enrichment analysis was conducted separately for upregulated and downregulated DEGs. For upregulated genes, the highest

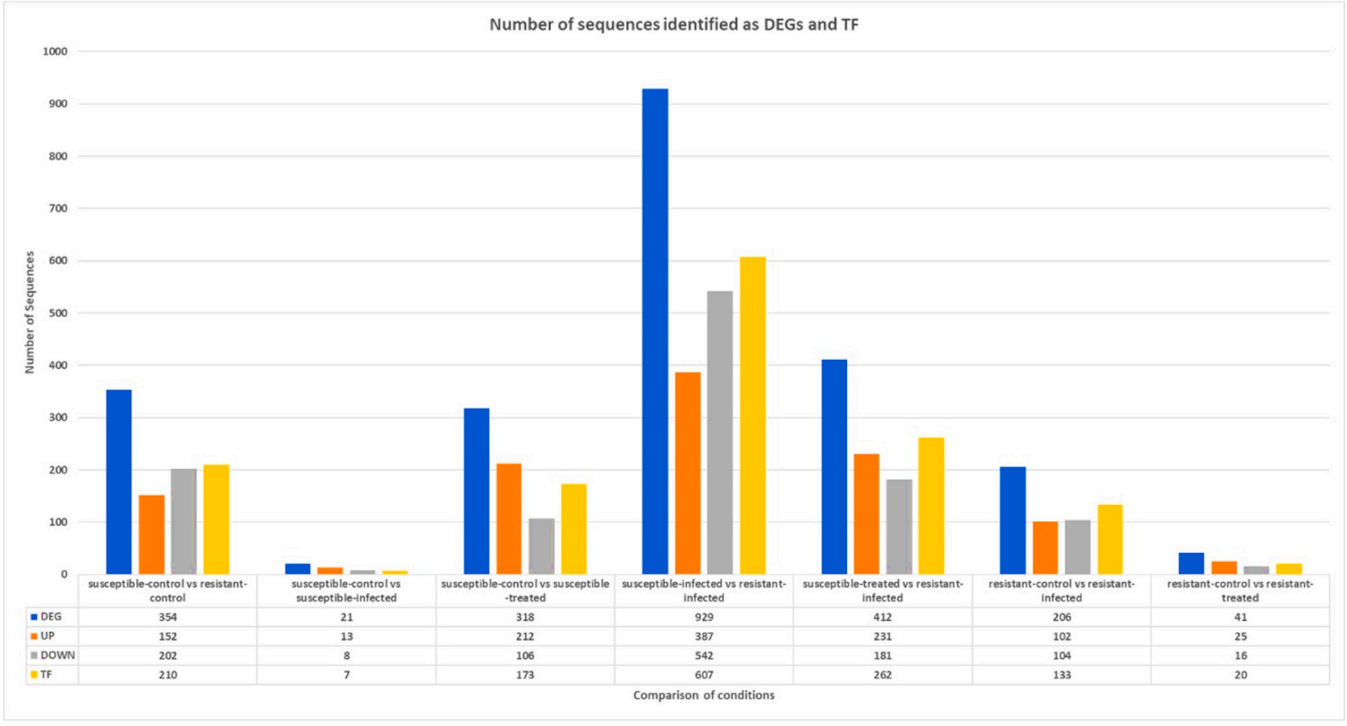

Fig. 5. Number of significant differentially expressed genes and Transcription Factors in various comparison sets.

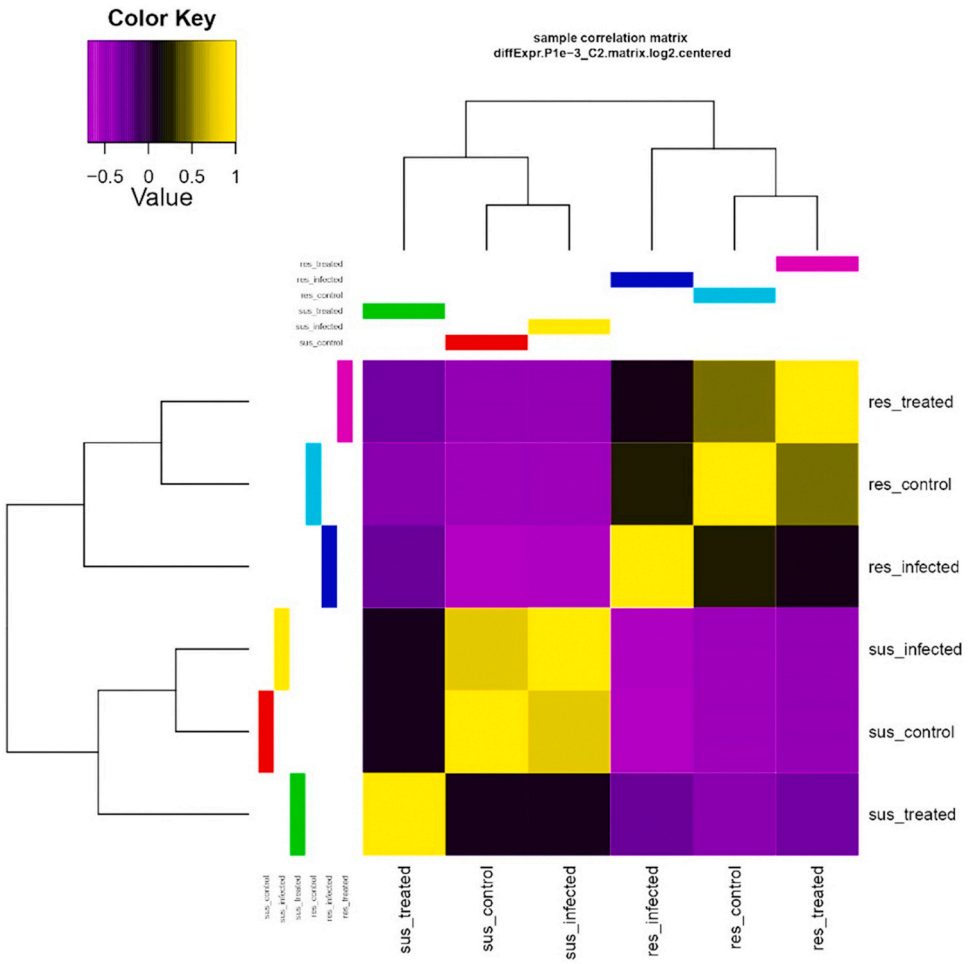

Fig. 6. Heatmap showing the hierarchically clustered Spearman correlation matrix resulting from comparing the transcript expression values for each of the 6 samples.

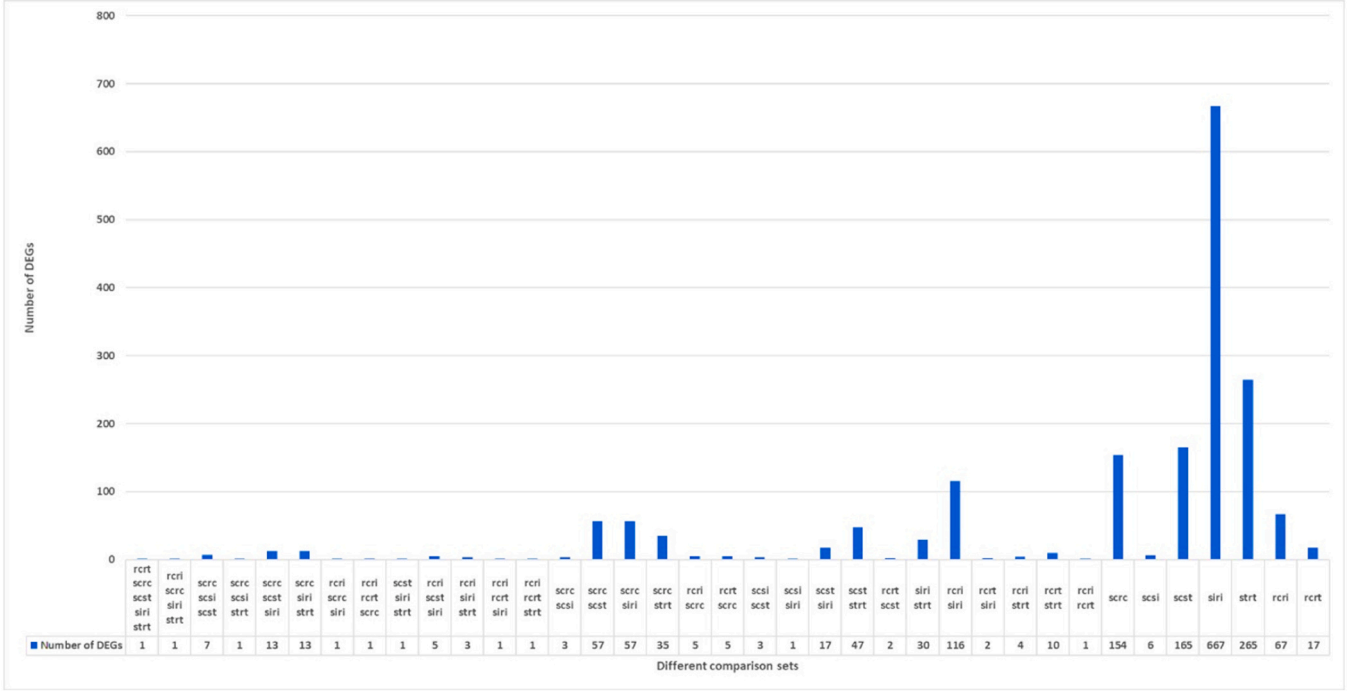

Fig. 7. A bar diagram showing the DEGs in each of the nine comparison sets. Some DEGs are shared between different comparison sets.

Table 1
Differentially expressed transcripts in response to charcoal rot disease.

SN	Gene ID	Description	Resistant infected	Susceptible infected
A. resistant infected and susceptible infected plants				
1	TRINITY_DN152677_c0_g3_i2	XP_003545772.1pathogenesis-related protein 1	Upregulated	Downregulated
2	TRINITY_DN157192_c1_g2_i4	NP_001236055.1stress-induced protein H4	Upregulated	Downregulated
3	TRINITY_DN163707_c2_g2_i2	NP_001235512.1disease resistance protein	Upregulated	Downregulated
4	TRINITY_DN157192_c1_g1_i4	XP_003543663.1 pleiotropic drug resistance protein 1	Upregulated	Downregulated
5	TRINITY_DN157572_c5_g4_i2	NP_001235031.1 BSP domain-containing protein precursor	Upregulated	Downregulated
6	TRINITY_DN163589_c2_g3_i2	XP_003551991.1protein NRT1/ PTR FAMILY 2.13	Upregulated	Downregulated
7	TRINITY_DN163688_c2_g6_i1	NP_001238536.1 receptor-like kinase	Upregulated	Downregulated
8	TRINITY_DN160984_c2_g4_i1	KHN03328.1 Major allergen Pru av 1	Upregulated	Downregulated
9	TRINITY_DN159419_c0_g1_i5	NP_001236953.2 dehydration responsive element-binding protein 3	Upregulated	Downregulated
10	TRINITY_DN157005_c0_g2_i1	NP_001238561.1chitinase class I precursor	Upregulated	Downregulated
11	TRINITY_DN154304_c2_g5_i2	XP_003528760.1 anthranilate N-methyltransferase	Upregulated	Downregulated
12	TRINITY_DN157352_c1_g2_i5	XP_003537598.1 isoflavone reductase	Upregulated	Downregulated
13	TRINITY_DN155040_c0_g1_i2	NP_001237509.1serine hydroxymethyltransferase 5	Upregulated	Downregulated
14	TRINITY_DN155388_c1_g1_i1	XP_028238106.1probable protein phosphatase 2 C 58	Upregulated	Downregulated
B. resistant infected and resistant treated plants				
1	TRINITY_DN153404_c1_g1_i4	XP_003551914.1trifunctional UDP-glucose 4,6-dehydratase/UDP−4-keto−6-deoxy-D-glucose 3,5-epimerase/UDP−4-keto-L-rhamnose-reductase RHM1	Upregulated	Downregulated
2	TRINITY_DN148173_c0_g1_i1	XP_028205173.1RNA-binding protein 12-like	Upregulated	Downregulated
3	TRINITY_DN154478_c0_g2_i4	NP_001238515.22-hydroxyisoflavanone synthase precursor	Upregulated	Downregulated
4	TRINITY_DN157192_c1_g2_i2	NP_001236038.1stress-induced protein SAM22	Upregulated	Downregulated
5	TRINITY_DN37574_c0_g1_i1	XP_003543246.1defensin-like protein	Upregulated	Downregulated
6	TRINITY_DN155588_c1_g7_i3	NP_001237911.1SRPBCC ligand-binding domain-containing protein	Upregulated	Downregulated
7	TRINITY_DN155028_c2_g4_i2	P10742.2RecName: Full=Stem 31 kDa glycoprotein; AltName: Full=Vegetative storage protein VSP25; Flags: Precursor	Downregulated	Upregulated
8	TRINITY_DN161100_c2_g6_i1	NP_001238401.1alpha-amylase inhibitor/lipid transfer/seed storage family protein precursor	Downregulated	Upregulated
9	TRINITY_DN153400_c0_g1_i6	XP_003522684.1BURPdomain protein RD22	Downregulated	Upregulated
10	TRINITY_DN162634_c2_g1_i9	XP_003531361.1inositol−3-phosphate synthase	Downregulated	Upregulated
11	TRINITY_DN162634_c2_g1_i7	XP_028233150.1inositol−3-phosphate synthase	Downregulated	Upregulated
12	TRINITY_DN155028_c2_g4_i2	P10742.2 Stem 31 kDa glycoprotein;	Downregulated	Upregulated
13	TRINITY_DN160334_c2_g2_i1	NP_001344954.1germin-like protein precursor	Downregulated	Upregulated
14	TRINITY_DN151581_c0_g1_i1	XP_028233150.1inositol−3-phosphate synthase	Downregulated	Upregulated
C. resistant infected and susceptible treated plants				
1	TRINITY_DN156371_c0_g3_i3	RZB79152.1Proline-rich protein 2 isoform B	Upregulated	Downregulated
2	TRINITY_DN156371_c0_g3_i8	KHN32307.1hypothetical protein glysoja_039170	Upregulated	Downregulated
3	TRINITY_DN156371_c0_g3_i7	RZB79153.1Proline-rich protein 2 isoform C	Upregulated	Downregulated
4	TRINITY_DN151231_c2_g1_i2	XP_006598120.3 repetitive proline-rich cell wall protein 1	Upregulated	Downregulated
5	TRINITY_DN151879_c0_g1_i5	XP_028237253.1 gibberellin-regulated protein 6-like	Upregulated	Downregulated
6	TRINITY_DN151879_c0_g2_i3	XP_003523021.1gibberellin-regulated protein 4	Upregulated	Downregulated
7	TRINITY_DN151231_c2_g1_i7	RZB66005.1 Foot protein 1 variant 1	Downregulated	Upregulated
8	TRINITY_DN161712_c4_g3_i1	XP_025982186.1uncharacterized protein LOC112999953	Downregulated	Upregulated
9	TRINITY_DN157794_c9_g2_i2	ACU16820.1unknown	Downregulated	Upregulated
10	TRINITY_DN163592_c0_g2_i1	YP_538810.1hypothetical chloroplast RF1	Downregulated	Upregulated
11	TRINITY_DN161448_c1_g2_i1	BAT88776.1hypothetical protein VIGAN_05238100, partial	Downregulated	Upregulated
12	TRINITY_DN154256_c2_g1_i7	YP_538774.1acetyl-CoA carboxylase carboxyltransferase beta subunit	Downregulated	Upregulated
13	TRINITY_DN163043_c1_g1_i1	XP_003516452.1programmed cell death protein 4	Downregulated	Upregulated

enrichment in the Biological Processes category was "lipid metabolic process" (GO:0005200) at 5.12 %. In Cellular Components, "extracellular regions" (GO:0005576) had the highest percentage at 5.71 %, followed by "vacuole" (GO:0004512) at 2.36 %. The top Molecular Function was "structural constituent of cytoskeleton" (GO:0006021) at 1.08 %. For downregulated genes, "transmembrane transport" (GO:0031347) was the most enriched Biological Process at 9.38 %, while "plasma membrane" was the only enriched Cellular Component at

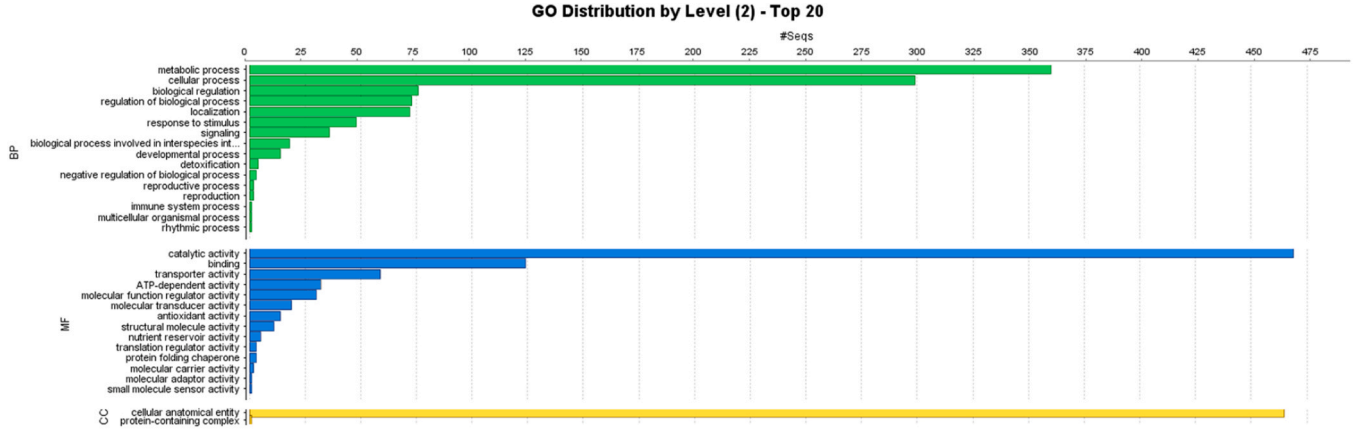

Fig. 8. GO distribution of DEGs.

10.68 %. The highest enrichment in Molecular Functions was "catalytic activity" at 13.53 %. Details are provided in Supplementary Fig. 4 and 5 and Supplementary Sheet 3. Kyoto Encyclopedia of Genes and Genomes (KEGG) pathway analysis showed that out of 354, 21, 318, 929, 412, 206, 41, 519, and 306 DEGs from nine comparisons, 22, 0, 21, 71, 23, 16, 2, 32, and 15 transcripts were assigned to one or more pathways, respectively. Many sequences were involved in sugar metabolism pathways, such as glycolysis/gluconeogenesis (map00010) and starch and sucrose metabolism (map00500) (Supplementary Sheet 4). Supplementary Fig. 6 displays the top 30 KEGG pathways identified in the DEGs. KEGG enrichment analysis revealed that the "Biosynthesis of ansamycins" (map01051) pathway is highly enriched (rich factor = 0.33), followed by "Flavone and flavonol biosynthesis" (map00944) (rich factor = 0.25) (Fig. 9 A). A total of 210, 7, 173, 607, 262, 133, 20, 359, and 191 transcription factors (TFs) were identified in the DEGs from the nine comparisons (Fig. 5). The most abundant sequences were associated with the ERF (Ethylene Responsive Factor) transcription factor, followed by the bHLH (helix-loop-helix) family. Other significant TFs identified include MYB, NAC, and FAR1 family proteins (Supplementary Sheet 5).

3.7. Variant identification

From the de novo assembled transcripts, a total of 111,447 putative SSRs were identified. Primers were successfully designed for 110,999 SSRs, while primers could not be designed for 448 SSRs. Among the SSRs with designed primers, 65,742 (59.22 %) were mononucleotides, 18,471 (16.64 %) were dinucleotides, 16,369 (14.74 %) were trinucleotides, 1185 (1.06 %) were tetranucleotides, 287 (0.25 %) were pentanucleotides, 193 (0.17 %) were hexanucleotides, and 8752 (7.88 %) were compound SSRs. Supplementary Sheet 6 provides details on all identified SSR markers and their primers. SNPs and InDels were identified in two contrasting varieties, resistant and susceptible. A total of 518,501 raw variants were detected in the resistant variety and 442,267 in the susceptible variety. The list of variants is available in Supplementary Sheet 7, and a circus plot of all variants is shown in Fig. 9B.

3.8. Gene regulatory networks

The top 50 genes (25 upregulated and 25 downregulated) from each of the nine sets were used to construct gene regulatory networks (GRNs), as shown in Supplementary Sheet 8. In the GRN, upregulated genes are marked in red, downregulated genes in blue, and potential hub genes in yellow. All gene networks are displayed in Supplementary Fig. 7 (a-i). Heatmaps were generated for all DEGs across the nine GRNs (Supplementary Fig. 8 (a-i)). These heatmaps can identify unique genes with a high fold change in a given comparison.

3.9. Soybean transcriptomics database

Data from the examination of transcriptomics were abundant. A website resource (STDbCr) has been created for soybean for the general public to utilize (http://backlin.cabgrid.res.in/stdbcr/). The database contains the actual transcripts that were created, differentially expressed genes (DEGs) identified across various comparison sets, transcription factors, and biomarkers such as simple sequence repeats (SSRs) and single nucleotide polymorphisms (SNPs) or insertions/deletions (InDels). The data is displayed in an interactive table that allows users to search and filter as needed.

The database currently contains 3106 DEGs across nine comparisons, 10,388 transcription factors, 110,999 SSRs, 518,501 variations in the resistant variety, and 442,267 variants in the susceptible variety. The user-friendly database allows for easy browsing of the data. A download section offers links to the original data submitted to NCBI, along with contact information. The RNAseq data is listed under the BioProject "The RNAseq Study on Charcoal Rot Fungal Disease in Soybean," with accession number PRJNA1026744 and ID 1026744. The data can be accessed following this link: (https://www.ncbi.nlm.nih.gov/bioproject/?term=PRJNA1026744)

3.10. Validation of DEGs by qRT-PCR

Quantitative real-time PCR of 8 randomly chosen DEGs was carried out to verify genes retrieved from RNA-seq data. The gene-specific

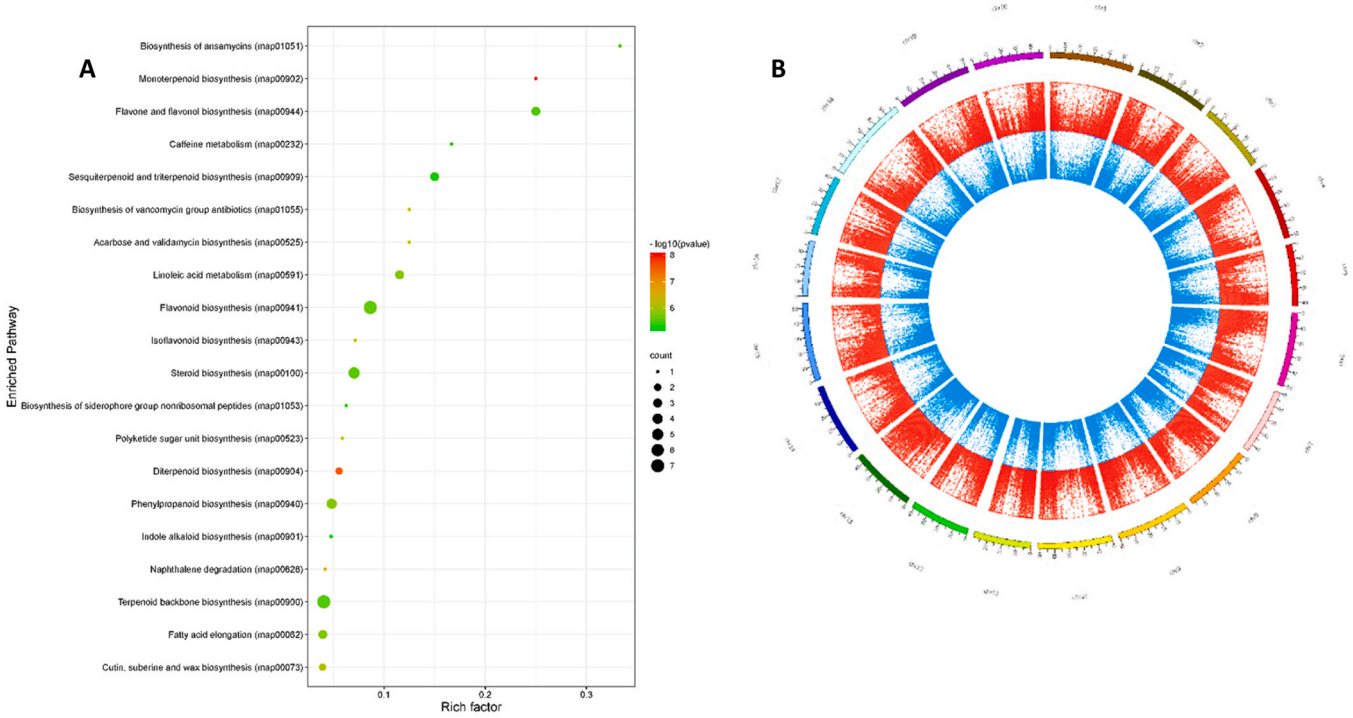

Fig. 9. A. KEGG pathway enrichment [20]. B. Circos plot of all the variants (ANP and INDEL) present in resistant (blue) and susceptible (red) variety.

primers were designed and examined in samples of soybean that were susceptible, resistant, treated, and untreated (Supplementary Table 3). The internal control Con-15 (a protein kinase related to CDPK) gene was utilized to normalize the amount of gene expression. The data of qRT PCR correlated with the RNA-seq results. All infected and treated samples showed elevated expression of the putative gene and (EUC67555.1) plant senescence-associated protein the treated samples showed high regulation of these genes (Fig. 10).

sc: susceptible control, si: susceptible infected, st: susceptible treated, rc: resistant control; ri: resistant infected, rt: resistant treated, HKG: house kipping gene.

The Ribosomal protein L16 (chloroplast) (YP 009309192.1) and hypothetical protein AGABI2DRAFT 187811 (XP 006455547.1) genes showed similar results in terms of upregulation of gene expression. Other randomly chosen DEGs whose expression was investigated for downregulation include the sucrose transport protein SUC2, the zinc finger protein ZAT10-like, the inositol-3-phosphate synthase, and the protein NRT1/PTR FAMILY (KHN32802.1, XP 028211725.1, and XP 003551991.1). 2.13 (Fig. 10). It was observed that the expression of DEGs examined by qRT PCR and RNA-seq data were both identical.

4. Discussion

This investigation provides a comprehensive transcriptomic analysis and small-scale experiments indicating that silicon treatment protect soybean plants from *Macrophomina phaseolina* infection by disrupting pathogen interactions with plant defense receptors. While previous research highlights silicon's role in combating various pathogens [1,25], its exact mechanism of action is not fully understood. The present investigation aims to bridge this gap, presenting the first RNA-Seq analysis of soybean's response to charcoal rot with a focus on silicon treatment.

Key findings include notable silicon accumulation in soybean trichomes, which may enhance leaf toughness and resistance to fungal penetration. Additionally, silicon deposition in root cell walls reinforces structural integrity, reducing fungal colonization. This aligns with similar studies on soybean rust, suggesting a potential universal silicon-mediated defense mechanism [34]. Previous studies also indicate silicon's role in enhancing cold tolerance and overall plant resilience [17, 2]. Previous studies [47,56] revealed that certain Arabidopsis plants, which were unable to use a specific defense pathway to protect against powdery mildew, still managed to resist the disease when treated with silicon (Si). This suggests that silicon plays a broader role beyond just enhancing plant disease resistance [31,51].

Notably, soybean plants treated with 1.7 mM K_2SiO_3 showed strong protection against *Macrophomina phaseolina.* This effect was further supported by transcriptome analysis, which revealed that gene expression in silicon-treated infected plants closely resembled that of healthy control plants. These findings are consistent with previous research [38], which showed that silicon-treated plants had a significant response against *Phytophthora sojae*. Similarly, other studies have demonstrated that silicon dioxide application reduces the severity of Asian Soybean Rust (ASR) and increases silicon accumulation in soybean leaf tissues [34]. This study examines the effect of potassium silicate on combating charcoal rot in soybean, identifying 3106 DEGs, including 1317 unique ones. The susceptible treated variety showed more DEGs than the resistant treated variety, likely due to pre-existing resistance genes. The treatment's effectiveness was evident from the significant DEG differences between the two groups. Previous studies suggest that silicon mainly supports plants under stress, which aligns with our findings. For instance, Rasoolizadeh et al. [38] observed that silicon had minimal effects on healthy soybean plants, influencing only around 50 out of 56, 000 genes during *Phytophthora sojae* infection, mostly through downregulation without specific pathway changes. This suggests silicon primarily offers protection during stress [22,31,39], a conclusion consistent with the present findings.

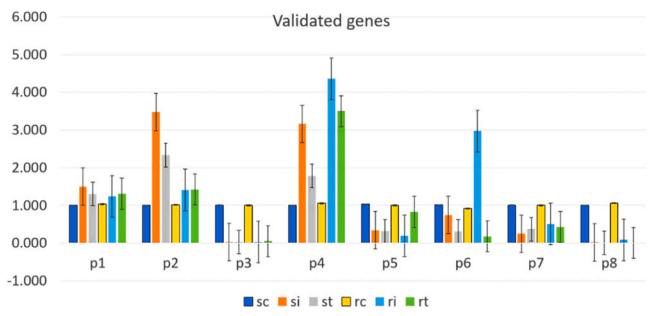

Fig. 10. Validation of differential expressed genes.

The silicon treatment influences various genes and proteins involved in the soybean plant's defense mechanisms [53]. The Fig. 11 illustrates the silicon-induced resistance pathway in soybean, showcasing how silicon modulates a network of pathways to enhance defense against *Macrophomina phaseolina*. This complex process involves activating genes responsible for structural reinforcement, stress response, and antimicrobial compound production, collectively strengthening the plant's resistance to the pathogen. Silicon upregulates genes involved in cell wall reinforcement, such as RHM1, enhancing structural barriers against pathogen invasion. Additionally, genes associated with the production of antimicrobial compounds like, RNA-binding protein 12-like, Defensin-like protein, Chitinase Class I Precursor and Pathogenesis-related Protein 1 (PR1 such as, β-1,3-glucanases destroy fungal β-1,3-glucans, and these enzymes prevent the proliferation of pathogens), are activated to target the pathogen directly. Silicon treatment also stimulates stress response genes, such as Stress-induced Protein H4 and Dehydration Responsive Element-Binding Protein 3 (DREB3), which activate signalling cascades for enhanced stress tolerance and defense. Silicon also influences genes related to stress responses, such as BURP domain protein RD22 and Stress-induced protein SAM22, which help mitigate charcoal rot stress through hormonal signalling (e.g., foot protein 1). Furthermore, silicon enhances the production of reactive oxygen species (ROS) and phytoalexins, vital for pathogen suppression, by regulating genes like 2-hydroxyisoflavanone synthase and Germin-like protein. Moreover, genes involved in programmed cell death and immune responses, such as Disease Resistance Protein are modulated to reduce pathogen proliferation and limit disease progression. These mechanisms collectively strengthen the plant's defense, reduce pathogen proliferation, and limit disease progression. A significant proportion of differentially expressed genes (DEGs) in the investigation were linked to ethylene-responsive factor (ERF), MYB, NAC, and FAR1 proteins, highlighting their sensitivity to treatment. The activation of ethylene pathways, known for triggering immune responses, often involves upregulation of Pathogenesis-related (PR) genes such as β-1,3-glucanase and chitinase [46,49,50]. This overexpression was observed in both resistant and susceptible silicon-treated plants, indicating an activated resistance mechanism against charcoal rot. Transcription factors such as MYB, NAC, and ERF are essential for defense, as they play a key role in activating PR proteins [13,48]. Consistent with previous findings [36,49,50], it revealed high expression of ERF proteins, particularly NP001235512 protein in resistant soybean genotype. Supporting studies include Patel et al. [35] and Ahmed et al. [3] reporting significant upregulation of callose synthase, PR genes, and receptor-like protein genes in *Lomandra longifolia* roots infected with *Phytophthora nicotianae*. Xiang et al. [52], who observed similar findings in apple roots infected with *Fusarium solani*, including differential expression of defense-related genes such as Cytochrome P450s and UDP-glycosyltransferases.

The current study identified elevated levels of the NAC family protein chitinase class-I precursor in both susceptible treated and resistant soybean genotypes, indicating its potential role in resistance. Previous research has linked ERF/AP2, CDPK, and leucine-rich repeats to soybean

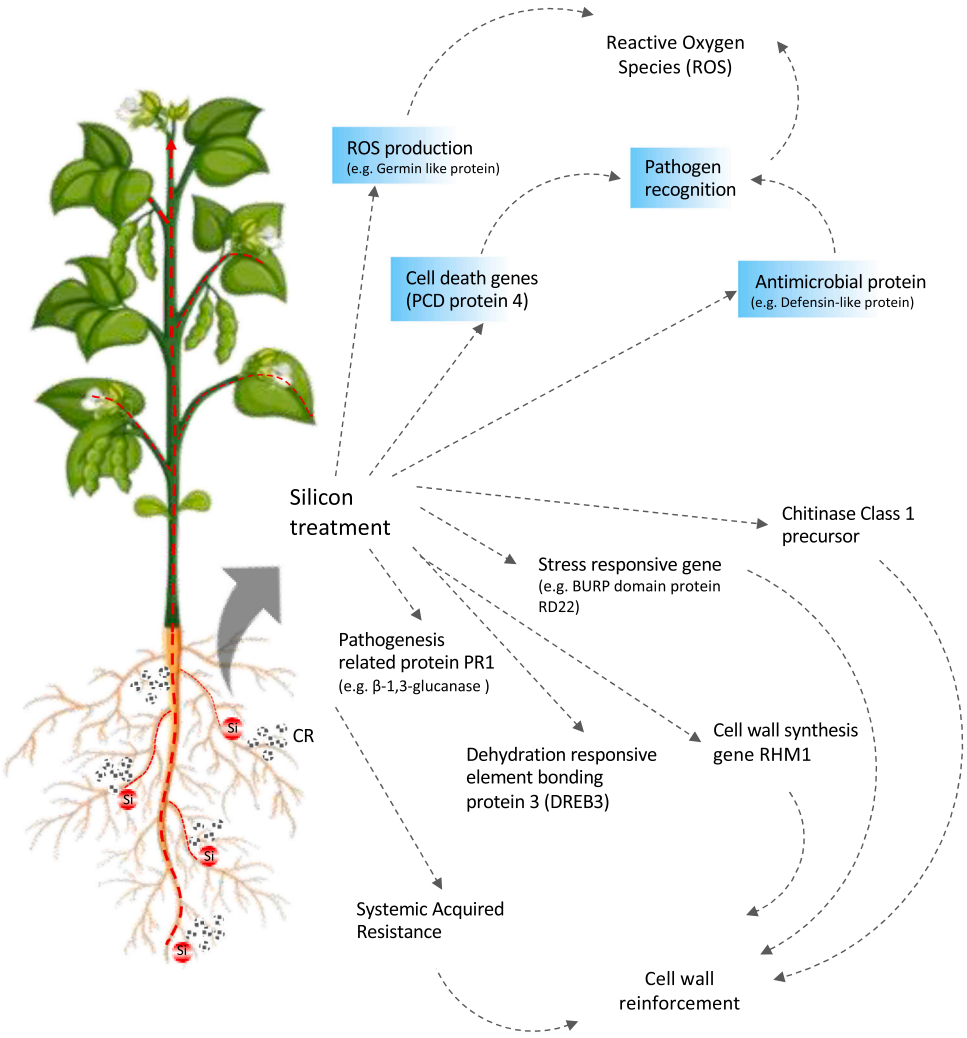

Fig. 11. Silicon-induced resistance pathway in soybean enhancing defense against *Macrophomina phaseolina*.

resistance to charcoal rot [55]. Genes such as the transcription factor ABR1, NRT1/PTR FAMILY protein, and LRR receptor-like serine/threonine-protein kinase showed elevated expression in resistant infected plants, highlighting their role in enhancing plant immunity [12]. Conversely, resistant infected plants exhibited downregulation of genes related to seed storage, lipid transport, and alpha-amylase inhibition, indicating a reduction in metabolic activities that support pathogen defense [26,54]. The current study revealed differential expression of genes encoding Leucine-Rich Repeat Receptor-Like Kinases and LRR domain genes, which respond to environmental cues and infections. Similarly, the NAC transcription factor family, known for its role in pathogen hypersensitivity, may activate chitinase to enhance resistance. Additionally, WRKY, NBs-LRR, and flavonoid pathways are implicated in charcoal rot resistance [11,37]. Present findings align with these reports, showing that genes related to these pathways including zinc finger proteins and ribosomal protein L16 are upregulated in both resistant and susceptible soybean genotypes treated with silicon. This suggests that these proteins could be involved in resistance mechanisms.

The KEGG enrichment analysis in the current study revealed significant enrichment in ansamycin biosynthesis, which supports plant growth under stress, as well as an increase in flavone and flavanol production. Silicon treatment enhanced defense mechanisms by promoting polyphenolic compound deposition, such as flavonoids, which help inhibit pathogen growth. Flavonoids and reactive oxygen species (ROS) act as stress protectors, while transcription factors (TFs) like MYB and bHLH activate defense pathways. It supports the role of MYB, bHLH, and WD40 TFs in regulating flavone and flavanol biosynthesis, with higher expression observed in resistant genotype.

The histopathological examination of roots from a susceptible soybean genotype infected with *Macrophomina phaseolina* in the present study revealed significant changes in cell structure. The fungus caused blockages in the vascular tissue and increased proliferation of microsclerotia over time. Real-time observation of hyphal penetration provided valuable visual evidence of the infection process (https://youtube.com/shorts/t1iT5Hic2_M?feature=share). Additionally, a resistant genotype was identified, showing significant suppression of hyphal penetration and growth. These findings align with Hemmati et al. [15], who reported similar effects on epidermal penetration, hyphal development, and microsclerotia attachment. The present findings illuminate the molecular mechanisms of *Macrophomina phaseolina* infection in soybean, offering insights for breeding resistant plants. Using the Illumina HiSeq platform, we identified 41 defense-related genes in the resistant genotype *versus* nine in the susceptible one. Further research is needed to pinpoint which of these genes confer resistance, involving CRISPR-Cas9 gene editing, proteomic analyses, and gene knockout or overexpression studies. These findings are a valuable resource for developing resistance strategies, though additional research is required to fully understand the roles of these genes.

5. Conclusion

This study explores how potassium silicate (1.7 mM K_2SiO_3)

improves soybean resistance to charcoal rot, significantly reducing the mortality rate of the susceptible genotype TAMS-38 from 69.7 % to 9 %. It identifies candidate genes associated with susceptibility and resistance to *Macrophomina phaseolina* in both resistant and susceptible genotypes, enhancing our understanding of the molecular mechanisms of host-pathogen interactions and the effects of silicon treatment. The transcriptomics data is made available in the STDbCr database [BioProject ID: PRJNA1026744] at https://www.ncbi.nlm.nih.gov/bioproject/?term=PRJNA1026744. These findings support strategies for combating charcoal rot and improving soybean resilience, offering valuable insights for breeding resistant varieties. Further validation through methods such as VIGS for transient gene silencing or CRISPR-Cas9 for gene knockout is needed to confirm these results and understand silicon's role in modifying the infection process and genetic responses.

Ethics approval and consent to participate

Not applicable.

Funding

The study was supported by the Dr. Panjabrao Deshmukh Krishi Vidyapeeth, Akola, Maharashtra State and Department of Biotechnology (DBT), Government of India, New Delhi under the project No. BT/PR30841AGIII/103/1112/2019.

Declaration of Generative AI and AI-assisted technologies in the writing process

No any AI-assisted technology is used in the writing process.

Declaration of Competing Interest

The authors declare the following financial interests/personal relationships which may be considered as potential competing interests: P. V. Jadhav reports financial support was provided by Department of Biotechnology (DBT), Government of India, New Delhi. If there are other authors, they declare that they have no known competing financial interests or personal relationships that could have appeared to influence the work reported in this paper.

Acknowledgements

The authors gratefully acknowledge the support from Dr. Panjabrao Deshmukh Krishi Vidyapeeth, Akola, Maharashtra, and the Department of Biotechnology (DBT), Government of India, New Delhi, under project No. BT/PR30841AGIII/103/1112/2019. Special thanks are extended to the ICAR-Indian Institute for providing the experimental material essential for this project.

Author contributions

Pravin Jadhav: Conceptualization, methodology and project administration and funding acquisition; **Sayali Magar:** Validation, Investigation, Writing Original Draft; **Parva Sharma:** Software; **Umesh Shinde:** Investigation, Writing Original Draft; **Eknath Vaidya**: Conceptualization, writing Original Draft, resource; **Sarika Jaiswal:** Software and Validation; **Satish Nichal:** Formal analysis; **Rajiv Ghawade:** Investigation; **Mir Asif Iquebal:** Software and Data Curation; **Prashant Kawar:** Validation; **Pritam Jadhav:** Validation; **Sanjay Sakhare:** Supervision; **Rupesh Deshmukh:** Data Curation; **Humira Sonah:** Formal analysis and Data Curation; **Dinesh Kumar:** Supervision; **Vineet Kumar:** Resource; **Vilas Kharche:** Resource and Project administration; **Shyamsunder Mane:** Methodology and Project administration

Adherence to national and international regulations

Not applicable.

Consent for publication

Not applicable.

Appendix A. Supporting information

Supplementary data associated with this article can be found in the online version at doi:10.1016/j.cpb.2025.100442.

Data availability

Data will be made available on request.

References

[1] G.J. Ahammed, Y. Yang, Mechanisms of silicon-induced fungal disease resistance in plants, Plant Physiol. Biochem. 165 (2021) 200–206.
[2] W. Ahmad, L. Coffman, A.D. Weerasooriya, K. Crawfordm, A.L. Khan, The silicon regulates microbiome diversity and plant defenses during cold stress in *Glycine max* L, Front. Plant Sci. 14 (2023) 1280251, https://doi.org/10.3389/fpls.2023.1280251.
[3] J. Ahmed, Y. Sajjad, M.K. Gatasheh, K.E. Ibrahim, M. Huzafa, S.A. Khan, C. Situ, A. M. Abbasi, A. Hassan, Genome-wide identification of NAC transcription factors and regulation of monoterpenoid indole alkaloid biosynthesis in *Catharanthus roseus*, Front. Plant Sci. 14 (2023) 1286584, https://doi.org/10.3389/fpls.2023.1286584.
[4] F. Almomani, M. Alhawatema, K. Hameed, Detection, identification and morphological characteristic of Macrophomina phaseolina: the charcoal rot disease pathogens isolated from infected plants in Northern Jordan, Arch. Phytopathol. Plant Prot. 46 (9) (2013) 1005–1014, https://doi.org/10.1080/03235408.2012.756174.
[5] P.K. Amrate, M.K. Shrivastava, M.S. Bhale, N. Agrawal, G. Kumawat, M. Shivakumar, V. Nataraj, Identification and genetic diversity analysis of high-yielding charcoal rot resistant soybean genotypes, Sci. Rep. 13 (2023) 8905, https://doi.org/10.1038/s41598-023-35688-2.
[6] Andrews, S., 2010. FastQC - A quality control tool for high throughput sequence data. ⟨http://www.bioinformatics.babraham.ac.uk/projects/fastqc/⟩. Babraham Bioinformatics. 2010.
[7] A.M. Bolger, M. Lohse, B. Usadel, Trimmomatic: a flexible trimmer for Illumina sequence data, 1, Bioinformatics 30 (15) (2014) 2114–2120, https://doi.org/10.1093/bioinformatics/btu170.
[8] C. Camacho, G. Coulouris, V. Avagyan, N. Ma, J. Papadopoulos, K. Bealer, T. L. Madden, BLAST+ : architecture and applications, BMC Bioinforma. 10 (2009) 421, https://doi.org/10.1186/1471-2105-10-421.
[9] A. Conesa, G. Stefan, Blast2GO: a comprehensive suite for functional analysis in plant genomics, Int. J. Plant Genom. ID 12 (2008) 619832, https://doi.org/10.1155/2008/619832;2008.
[10] M.P. da Silva, M. Klepadlo, E.E. Gbur, A. Pereira, R.E. Mason, J.C. Rupe, B. H. Bluhm, L. Wood, L.A. Mozzoni, P. Chen, QTL mapping of charcoal rot resistance in PI 567562A soybean accession, Crop Sci. 59 (2019) 474–479, https://doi.org/10.2135/cropsci2018.02.0145.
[11] R. Deshmukh, S. Tiwari, Molecular interaction of charcoal rot pathogenesis in soybean: a complex interaction, 2021, Plant Cell Rep. 40 (10) (2021) 1799–1812, https://doi.org/10.1007/s00299-021-02747-9.
[12] C. dos Santos, O.L. Franco, Pathogenesis-related proteins (PRs) with enzyme activity activating plant defense responses, Plants 12 (11) (2023) 2226, https://doi.org/10.3390/plants12112226.
[13] C. Fu, M.Y. Liu, Genome-wide identification and molecular evolution of NAC gene family in Dendrobium nobile, Front. Plant Sci. 14 (2023) 1232804, https://doi.org/10.3389/fpls.2023.1232804.
[14] B.J. Haas, A. Papanicolaou, M. Yassour, M. Grabherr, P.D. Blood, J. Bowden, M. B. Couger, D. Eccles, M. Lieber, M.D. MacManes, M. Ott, J. Orvis, N. Pochet, F. Strozzi, N. Weeks, R. Westerman, T. William, C.N. Dewey, R. Henschel, R. D. LeDuc, N. Friedman, A. Regev, De novo transcript sequence reconstruction from RNA-seq using the Trinity platform for reference generation and analysis, Nat. Protoc. 8 (2013) 1494–1512, https://doi.org/10.1038/nprot.2013.084.
[15] P. Hemmati, D. Zafari, S.B. Mahmoodi, M. Hashemi, M. Gholamhoseini, A. Dolatabadian, R. Ataei, Histopathology of charcoal rot disease (*Macrophomina phaseolina*) in resistant and susceptible cultivars of soybean, Rhizosphere 7 (2018) 27–34.
[16] S. Huang, L. Pu, G. He, X. Wang, D. Chen, X. Xie, L. Qie, Y. Dan, R. Zhang, Z. Gong, Y. Lu, Silicon in soil and its interaction with nitrogen, phosphorus, and potassium nutrients on rice yield: a case study of paddy fields in the Taihu Lake region, China, without a history of silicon fertilization, Soil Tillage Res 238 (2024) 106027, https://doi.org/10.1016/j.still.2024.106027.
[17] B. Hussain, L. Riaz, K. Li, K. Hayat, N. Akbar, M.Z. Hadeed, B. Zhu, S. Pu, Abiogenic silicon: Interaction with potentially toxic elements and its ecological significance in

soil and plant systems, 1, Environ. Pollut. 338 (2023) 122689, https://doi.org/10.1016/j.envpol.2023.122689.
[18] S. Jaiswal, P.V. Jadhav, R.S. Jasrotia, P.B. Kale, S.K. Kad, M.P. Moharil, M. S. Dudhare, J. Kheni, A.G. Deshmukh, S.S. Mane, R.S. Nandanwar, S. Penna, J. G. Manjaya, M.A. Iquebal, R.S. Tomar, P.G. Kawar, A. Rai, D. Kumar, Transcriptomic signature reveals mechanism of flower bud distortion in witches'-broom disease of soybean (*Glycine max*), BMC Plant Biol. 19 (2019) 26, https://doi.org/10.1186/s12870-018-1601-1.
[19] X. Jin, H. Huang, L. Wang, Y. Sun, S. Dai, Transcriptomics and metabolite analysis reveals the molecular mechanism of anthocyanin biosynthesis branch pathway in different senecio cruentus cultivars, Front. Plant Sci. 7 (2016) 1307, https://doi.org/10.3389/fpls.2016.01307.
[20] M. Kanehisa, S. Goto, 2000. KEGG: Kyoto Encyclopedia of Genes and Genomes, Nucleic Acids Res. 28:27–30, Nucleic Acids Res 28 (2000) 27–30, https://doi.org/10.1093/nar/28.1.27.
[21] S. Kaur, G.S. Dhillon, S.K. Brar, G.E. Vallad, R. Chand, V.B. Chauhan, Emerging phytopathogen *Macrophomina phaseolina*: biology, economic importance and current diagnostic trends, Crit. Rev. Microbiol. 38 (2) (2012) 136–151, https://doi.org/10.3109/1040841X.2011.640977.
[22] L. Koleva, A. Umar, N.A. Yasin, A.A. Shah, M.H. Siddiqui, S. Alamri, L. Riaz, A. Raza, T. Javed, Z. Shabbir, Iron oxide and silicon nanoparticles modulate mineral nutrient homeostasis and metabolism in cadmium-stressed phaseolus vulgaris, Front. Plant Sci. 13 (2022) 806781, https://doi.org/10.3389/fpls.2022.806781.
[23] B. Langmead, S.L. Salzberg, Fast gapped-read alignment with Bowtie 2, Nat. Methods 9 (2012) 357–359, https://doi.org/10.1038/nmeth.1923.
[24] B. Li, C.N. Dewey, RSEM: accurate transcript quantification from RNA-Seq data with or without a reference genome, BMC Bioinforma. 12 (2011) 323, https://doi.org/10.1186/1471-2105-12-323.
[25] R. Li, Y. Sun, H. Wang, H. Wang, Advances in understanding silicon transporters and the benefits to silicon-associated disease resistance in plants, Appl. Sci. 12 (7) (2022) 3282, https://doi.org/10.3390/app12073282.
[26] H. Li, Y. Zhang, Z. Liu, C. Guo, M. Battino, S. Cai, J. Yi, Exploring antioxidant activities and inhibitory effects against α-amylase and α-glucosidase of Elaeocarpus braceanus fruits: insights into mechanisms by molecular docking and molecular dynamics, Int. J. Food Sci. Technol. 59 (2024) 343–355, https://doi.org/10.1111/ijfs.16815.
[27] M. Libault, S. Thibivilliers, D.D. Bilgin, O. Radwan, M. Benitez, S.J. Clough, G. Stacey, Identification of four soybean reference genes for gene expression normalization, Plant Genome 1 (2008) 44–54, https://doi.org/10.3835/plantgenome2008.02.0091.
[28] K.J. Livak, T.D. Schmittgen, Analysis of relative gene expression data using real-time quantitative PCR and the 2-ΔΔCT method, Methods 25 (4) (2001) 402–408, https://doi.org/10.1006/meth.2001.1262.
[29] R. Mandlik, V. Thakral, G. Raturi, S. Shinde, M. Nikolić, D.K. Tripathi, H. Sonah, R. Deshmukh, Significance of silicon uptake, transport, and deposition in plants, J. Exp. Bot. 71 (21) (2020) 6703–6718, https://doi.org/10.1093/jxb/eraa301.
[30] A. Mengistu, J.D. Ray, J.R. Smith, P.R. Arelli, N. Bellaloui, P. Chen, G. Shannon, D. Boykin, Effect of charcoal rot on selected putative drought tolerant soybean genotypes and yield, Crop Prot. 105 (2018) 90–101, https://doi.org/10.1016/j.cropro.2017.11.012.
[31] V. Misra, A.K. Mall, S.A. Ansari, A. Raheem, M.K. Tripathi, M.I. Ansari, Silicon as a beneficial nutrient for productivity augmentation and abiotic/biotic stress tolerance in sugarcane, Biocatal. Agric. Biotechnol. 54 (3) (2023) 102944, https://doi.org/10.1016/j.bcab.2023.102944.
[32] L.C.M. Nidumolu, K.M. Lorilla, I. Chakravarty, C. Uhde-Stone, Soybean Root Transcriptomics: Insights into Sucrose Signaling at the Crossroads of Nutrient Deficiency and Biotic Stress Responses, Plants 12 (11) (2023) 2117, https://doi.org/10.3390/plants12112117.
[33] T. Nobori, A. Monell, A. Travis, Jingtian Lee, Zhou, R. Joseph, Nery, R. Joseph, Ecker, Time-resolved single-cell and spatial gene regulatory atlas of plants under pathogen attack, bioRxiv (2023), https://doi.org/10.1101/2023.04.10.536170.
[34] M.G. Otolakoski, B.G. Viegas, B.Z. Bagio, M.M.C. Blum, C.S. Suzana-Milan, J. Huzar-Novakowiski, Reduction of the severity of Asian soybean rust with foliar application of silicon dioxide, Crop Prot. 173 (2023) 106387, https://doi.org/10.1016/j.cropro.2023.106387.
[35] S. Patel, J. Patel, K. Bowen, J. Koebernick, Deciphering the genetic architecture of resistance to Corynespora cassiicola in soybean (*Glycine max* L.) by integrating genome-wide association mapping and RNA-Seq analysis, Front. Plant Sci. 14 (2023) 1255763, https://doi.org/10.3389/fpls.2023.1255763.
[36] M.R. Pimenta, P.A. Silva, G.C. Mendes, J.R. Alves, H.D.N. Caetano, J.P.B. Machado, O.J.B. Brustolini, P.A. Carpinetti, B.P. Melo, J.C.F. Silva, G.L. Rosado, M.F. S. Ferreira, M. Dal-Bianco, E.A. de Toledo Picoli, F.J.L. Aragao, H.J.O. Ramos, E.P. B. Fontes, The stress-induced soybean NAC transcription factor GmNAC81 plays a positive role in developmentally programmed leaf senescence, Plant Cell Physiol. 57 (5) (2016) 1098–1114, https://doi.org/10.1093/pcp/pcw059.
[37] N. Radadiya, N. Mangukia, V. Antala, H. Desai, H. Chaudhari, T.L. Dholaria, R. S. Tomar, B.A. Golakiya, M.K. Mahatma, Transcriptome analysis of sesame-*Macrophomina phaseolina* interactions revealing the distinct genetic components for early defense responses, Physiol. Mol. Biol. Plants 27 (8) (2021) 1675–1693, https://doi.org/10.1007/s12298-021-01039-6.
[38] A. Rasoolizadeh, C. Labbé, H. Sonah, R.K. Deshmukh, F. Belzile, J.G. Menzies, R. R. Bélanger, Silicon protects soybean plants against Phytophthora sojae by interfering with effector-receptor expression, BMC Plant Biol. 18 (2018) 97, https://doi.org/10.1186/s12870-018-1312-7.
[39] M.A.S. Raza, B. Zulfiqar, R. Iqbal, M.N. Muzamil, M.U. Aslam, F. Muhammad, J. Amin, H.M.U. Aslam, M.A. Ibrahim, M. Uzair, M. Habib-ur-Rahman, Morpho-physiological and biochemical response of wheat to various treatments of silicon nano-particles under drought stress conditions, Sci. Rep. 13 (2023) 2700, https://doi.org/10.1038/s41598-023-29784-6.
[40] M.D. Robinson, D.J. McCarthy, G.K. Smyth, edgeR: a Bioconductor package for differential expression analysis of digital gene expression data, Bioinform 26 (1) (2009) 139–140, https://doi.org/10.1093/bioinformatics/btp616.
[41] M. Sahebi, M.M. Hanafi, S.N.A. Akmar, M.Y. Rafii, P. Azizi, F.F. Tengoua, J.N. M. Azwa, M. Shabanimofrad, Importance of silicon and mechanisms of biosilica formation in plants, Biomed. Res. Int. 2015 (2015) 396010, https://doi.org/10.1155/2015/396010.
[42] B. Sharma, K.C. Kumawat, S. Tiwari, A. Kumar, R.A. Dar, U. Singh, M. Cardinale, Silicon and plant nutrition—dynamics, mechanisms of transport and role of silicon solubilizer microbiomes in sustainable agriculture: a review, Pedosphere 33 (4) (2023) 534–555, https://doi.org/10.1016/j.pedsph.2022.11.004.
[43] M. Shirai, T. Eulgem, Molecular interactions between the soilborne pathogenic fungus *Macrophomina phaseolina* and its host plants, Front. Plant Sci. 14 (2023) 1264569, https://doi.org/10.3389/fpls.2023.1264569.
[44] A. Shoaib, H. Ali, A. Javaid, Z.A. Awan, Contending charcoal rot disease of mungbean by employing biocontrol *Ochrobactrum ciceri* and zinc, Physiol. Mol. Biol. Plants 26 (7) (2020) 1385–1397, https://doi.org/10.1007/s12298-020-00817-y.
[45] R. Sinha, V. Irulappan, B. Mohan-Raju, A. Suganthi, M. Senthil-Kumar, Impact of drought stress on simultaneously occurring pathogen infection in field-grown chickpea, 3, Sci. Rep. 9 (1) (2019) 5577, https://doi.org/10.1038/s41598-019-41463-z.
[46] S.D. Thakur, P. Singh, S. Singh, A. Sasmal, T. Deb, S. Karmakar, T. Dasgupta, S. Sarkar, S. Sarkar, B. Ghosh, S. Ghosh, View of role of pathogenesis-related (PR) proteins in plant microbes defence mechanism, J. Surv. Fish. Sci. 10 (1S) (2023) 6344–6352.
[47] J. Vivancos, C. Labbé, J.G. Menzies, R.R. Bélanger, Silicon-mediated resistance of Arabidopsis against powdery mildew involves mechanisms other than the salicylic acid (SA)-dependent defence pathway, Mol. Plant Pathol. 16 (6) (2015) 572–582, https://doi.org/10.1111/mpp.12213. Epub 2014 Dec 15.
[48] Z. Wang, Z. Chen, Y. Wu, M. Mu, J. Jiang, W. Nie, S. Zhao, G. Cui, X. Yin, Genome-wide identification and characterization of NAC transcription factor family members in Trifolium pratense and expression analysis under lead stress, BMC Genom. 25 (2024) 128, https://doi.org/10.1186/s12864-023-09944-8.
[49] J. Wang, R. Li, Z. Zhao, M. Zhu, Y. Wang, Supporting Information Bioactivity, uptake and distribution of prothioconazole loaded on fluorescent double hollow shelled mesoporous silica in soybean plants, J. Agric. Food Chem. 71 (11) (2023) 4521–4535, https://doi.org/10.1021/acs.jafc.3c00200.
[50] Z. Wang, Z. Zhang, P. Wang, C. Qin, L. He, L. Kong, W. Ren, X. Liu, W. Ma, Genome-wide identification of the NAC transcription factors family and regulation of metabolites under salt stress in *Isatis indigotica*, Int. J. Biol. Macromol. 240 (2023) 124436, https://doi.org/10.1016/j.ijbiomac.2023.124436.
[51] K.T. Win, S. Maeda, M. Kobayashi, C.J. Jiang, Silicon enhances resistance to red crown rot caused by *Calonectria ilicicola* in Soybean, Agronomy 11 (5) (2021) 899, https://doi.org/10.3390/agronomy11050899.
[52] L. Xiang, M. Wang, F. Pan, G. Wang, W. Jiang, Y. Wang, X. Chen, C. Yin, Z. Mao, Transcriptome analysis Malus domestica 'M9T337' root molecular responses to Fusarium solani infection, Physiol. Mol. Plant Pathol. 113 (2021) 101567, https://doi.org/10.1016/j.pmpp.2020.101567.
[53] A.A. Younis, H. Khattab, M.M. Emam, Impacts of silicon and silicon nanoparticles on leaf ultrastructure and tapip1 and tanip2 gene expressions in heat stressed wheat seedlings, 2020, Biol. Plant. 64 (2020) 343–352, https://doi.org/10.32615/bp.2020.030.
[54] Q. Yu, Y. Tian, L. Fan, Inhibition mechanisms of wounded okra on the α-glucosidase/α-amylase, Food Biosci. 51 (2023) 102333, https://doi.org/10.1016/j.fbio.2022.102333.
[55] X. Yuan, H. Wang, J. Cai, D. Li, F. Song, NAC transcription factors in plant immunity, Phytopathol. Res 1 (2019) 3, https://doi.org/10.1186/s42483-018-0008-0.
[56] M. Yuvaraj, R. Sathya Priya, N. Jagathjothi, M. Saranya, N. Suganthi, R. Sharmila, J. Cyriac, R. Anitha, K.S. Subramanian, Silicon nanoparticles (SiNPs): challenges and perspectives for sustainable agriculture, Physiol. Mol. Plant Pathol. 128 (2023) 102161, https://doi.org/10.1016/j.pmpp.2023.102161.